



NAGI-1486

11-27-212-

0-7022

NASA/CR-96-

207308

## **AIAA 96-1967**

### **Frequency Response of Pressure Sensitive Paints**

N. A. Winslow, B. F. Carroll and F. M. Setzer  
University of Florida  
Gainesville, FL

## **27th AIAA Fluid Dynamics Conference**

**June 17-20, 1996 / New Orleans, LA**

# FREQUENCY RESPONSE OF PRESSURE SENSITIVE PAINTS

Neal A. Winslow,<sup>\*</sup> Bruce F. Carroll,<sup>†</sup> Fred M. Setzer<sup>‡</sup>

Department of Aerospace Engineering, Mechanics & Engineering Science  
University of Florida  
Gainesville, FL

## Abstract

An experimental method for measuring the frequency response of Pressure Sensitive Paints (PSP) is presented. These results lead to the development of a dynamic correction technique for PSP measurements which is of great importance to the advancement of PSP as a measurement technique. The ability to design such a dynamic corrector is most easily formed from the frequency response of the given system. An example of this correction technique is shown. In addition to the experimental data, an analytical model for the frequency response is developed from the one-dimensional mass diffusion equation.

## Nomenclature

$n$	=	oxygen concentration in PSP layer
$x$	=	distance above metal base
$t$	=	time
$D_m$	=	mass diffusivity
$a$	=	PSP layer thickness
$a_0$	=	primer layer thickness
$\omega$	=	driving frequency
$\tilde{x}$	=	distance above primer layer
$\beta_k$	=	parameter in mass diffusion solution
$\tau$	=	PSP lifetime
$\bar{n}$	=	average oxygen concentration in the PSP layer
$A$	=	Fourier amplitude spectrum
$f$	=	frequency
$\phi$	=	Fourier phase spectrum
$h$	=	transfer function
$M$	=	total number of points in transfer function sequence

$\mathfrak{F}$	=	Fourier transform
$m$	=	number of points used in transfer function sequence
$P_t$	=	"True" pressure measured from conventional pressure transducer
$P_c$	=	Corrected PSP pressure
$P_{PSP}$	=	PSP indicated pressure

## Introduction

Pressure Sensitive Paints (PSP) are gaining wide acceptance as a global pressure measuring system for steady state conditions.<sup>1-3</sup> However, the application of PSP to unsteady conditions is only now being attempted and is complicated by the inherently slow response of common PSP formulations. The dynamic characteristics of a PSP based measurement system can conveniently be studied in the time-domain (time response) or the frequency-domain (frequency response). The term dynamic response will be used to refer to the general response of PSP's to unsteady pressures and encompasses both the time and frequency domains. This paper focuses on the frequency response of several typical PSP coatings using Fourier methods. The advantage of viewing PSP behavior in the frequency domain is that it simplifies the analysis of complicated unsteady pressure fields and leads directly to dynamic compensation techniques.

The dynamic response of typical PSP coatings is limited by the mass diffusion rates of oxygen through the binder layer.<sup>4</sup> Two main approaches have been used to improve the PSP dynamic response: first to develop a coating with an extremely high mass diffusivity and second, to develop coatings with the probe molecules concentrated on the outer surface of the paint. Experimental results based on the first approach have been reported by Baron, et al.<sup>5</sup> Unfortunately, these "fast" formulations are not always suitable for wind tunnel testing due to high surface roughness and questionable durability. A formulation based on

<sup>\*</sup>Graduate Assistant, Student Member

<sup>†</sup>Associate Professor, Member

<sup>‡</sup>Undergraduate Assistant, Student Member

the second approach was characterized by Carroll, et al.,<sup>4</sup> who observed that the "fast paint" had a complex temporal behavior with overall response inferior to a standard formulation.

Given the inherently slow response of current PSP formulations and the limited success of formulating faster coatings, it is imperative that a thorough understanding of the dynamic characteristics of PSP formulations be developed before unsteady PSP pressure measurements can be obtained. Once the dynamic behavior of PSP coatings is understood, then dynamic compensation techniques may be developed to correct the time lag. Both Baron, et al. and Carroll, et al. performed time response characterizations of the coatings by looking at a step change in pressure.<sup>4,5</sup> However, due to the inherent shot noise of a PMT used as a measurement device, the pressure values obtained in these experiments tended to have large uncertainty. If a technique could be developed which would reduce the uncertainty in the experiment, the characterizations of the paints could be determined more accurately. The obvious manner for reducing these errors would be to average over several experimental runs. This leads to the idea of using a periodic signal so that the statistics could be built up over time. From here the transition to analysis of the frequency response is easily made.

### Experimental Setup

The setup of the experiments presented is very standard for the measurement of PSP's. It consists of a lamp to illuminate the PSP sample, a photomultiplier tube (PMT) for measuring the light output of the sample, a test cell containing the sample, and various optics. A schematic of this setup is contained in Fig. 1. The lamp is a tungsten-halogen lamp and is powered by a constant-current power supply with photofeedback to produce an extremely stable light intensity. The PMT is a system made up of the photomultiplier tube, power supply, and amplifier. The photomultiplier tube's range is between 185 nm and 900 nm. There are two filters in use in the experiment. The first is attached to the lamp and is a bandpass filter centered at 450 nm with a full-width-at-half-max (FWHM) of 40 nm. The second is immediately before the light from the sample enters the PMT and is also a bandpass filter but is centered at 650 nm with a FWHM of 90 nm. The filters used here are such that there is no overlap between the excitation

wavelength and the emission wavelength. A standard optical mirror is used to redirect the light from the lamp into the test cell. A lens is used to focus the light from the sample onto the PMT. The test cell, shown in Fig. 2, is specially designed for the investigation of the response of PSP's to pressure as well as temperature changes. It is hexagonal in shape with six ports entering into the volume above the sample. The back end of the cell holds a cylindrical volume into which temperature controlled water can be circulated. The PSP sample has dimensions 1.27 x 1.59 cm of which approximately 1.3 cm<sup>2</sup> can be viewed. A side view of the PSP sample is shown in Fig. 3. A typical sample consists of an aluminum base over which a layer of primer paint is laid. The PSP layer is then applied on top of the primer layer. The primer layer is on the order of 10  $\mu$ m thick and the PSP layer ranges between 5 and 30  $\mu$ m. The thickness of the layers is measured using a nondestructive eddy current gauge. The PSP itself consists of a proprietary ruthenium based dye dispersed in a silicone polymer binder. The PSP sample is separated from a glass window by a small volume 0.32 cm thick and 1.27 cm in diameter. Of the six ports, only four were necessary for the experiments presented here. The first is connected to vacuum which is continuously drawing on the control volume. The second is connected to a high pressure of 200 kPa via an analog valve. This valve opens proportional to the amount of voltage applied. When controlled via an output from a D/A board, it allows for the creation of arbitrary pressure field functions. The third is connected to a conventional pressure transducer with a useful frequency range of 500 kHz. The fourth is connected to an electronic manometer used for calibration purposes. A valve to the manometer can be shut after calibration to minimize the volume. The two remaining ports are available for the insertion of devices to measure the temperature of the sample. The voltages from the pressure transducer and PMT each go through analog filtering before going to the A/D board. These filters are first order lowpass filters with a cutoff frequency of 480 Hz. The filtered signals are then sampled at a rate of between 10 and 200 Hz and digitized to 12 bits. Calibration of the PSP and pressure transducer are performed by cracking open the analog valve, waiting for the PSP to equilibrate, and then recording the voltages of the PMT and pressure transducer signals and the pressure at the manometer. Then, the valve is cracked open a little more and the process is repeated. Twenty calibration points are taken between the valve being

completely closed and completely open. The pressure as a function of PMT voltage is fit with a 4<sup>th</sup> order polynomial and the transducer calibration data are fit to a straight line.

### Theory

The photochemical processes upon which PSP is based have been adequately described in previous works, and will not be repeated here.<sup>1-3</sup> Suffice to say that PSP takes advantage of oxygen quenching of a luminescent dye dispersed in an oxygen permeable binder. As the pressure above the layer increases, the equilibrium oxygen concentration within the layer increases leading to a lower luminescence intensity. To understand the dynamic characteristics of PSP we must first look at the diffusion of oxygen within the layer.

The first step in investigating the frequency response characteristics of PSP's is to develop an analytical model to predict the behavior of the paints. The model developed here is identical to the model used by Carroll, et. al. with the exception of the boundary conditions at the upper and lower surfaces of the coating.<sup>4</sup> Rather than applying a step rise in pressure, a sinusoidally varying pressure field is applied. The model is defined as follows,

$$\frac{\partial^2 n(x,t)}{\partial x^2} = \frac{1}{D_m} \frac{\partial n(x,t)}{\partial t} \quad (1)$$

$$n(a_0 + a, t) = n_0 + n_1 \sin(\omega t) \quad (2)$$

$$\frac{\partial n(a_0, t)}{\partial x} = 0 \quad (3)$$

$$n(x, 0) = n_0 \quad (4)$$

where  $n$  is the oxygen concentration at depth  $x$  and time  $t$ ,  $D_m$  is the mass diffusivity of the PSP layer, and  $\omega$  is the driving frequency of the sine wave. The constant  $n_0$  represents the mean oxygen concentration and  $n_1$  is the amplitude of the fluctuation about that mean. Equation (1) which is the governing differential equation is simply the one-dimensional mass diffusion equation. Equations (2) and (3) describe the boundary conditions at the upper and lower interfaces of the PSP layer. Equation (4) is the initial condition of the PSP layer. The geometry of the problem is as shown previously in Fig. 3. If a change of variables is made by letting  $\tilde{x} = x - a_0$ , an analytical solution can be reached for

the oxygen concentration in the PSP layer as a function of time.

$$n(\tilde{x}, t) = n_0 + n_1 \frac{4}{\pi} \sum_{k=1}^{\infty} \frac{(-1)^{k-1}}{(2k-1)} \cos\left[\frac{(2k-1)\pi\tilde{x}}{2a}\right] \sin(\omega t - \beta_k) \cos(\beta_k) \quad (5)$$

where

$$\beta_k = \tan^{-1} \left[ \frac{\omega \tau}{(2k-1)^2} \right] \quad (6)$$

and

$$\tau = \frac{4a^2}{\pi^2 D_m} \quad (7)$$

It should be noted that the above solution is for time approaching infinity so that all transients have been damped out. If we then average across the thickness of the PSP layer:

$$\begin{aligned} \bar{n}(t) &= \frac{1}{a} \int_0^a n(\tilde{x}, t) d\tilde{x} \\ &= n_0 + n_1 \left[ \frac{1}{2} \sin(\omega t) + \frac{4}{\pi^2} \sum_{k=1}^{\infty} \frac{\sin(\omega t - 2\beta_k)}{(2k-1)^2} \right] \end{aligned} \quad (8)$$

we have the average oxygen concentration in the layer as a function of time. Note that we have assumed that a unit area of PSP is being considered. We can non-dimensionalize the input oxygen concentration of Eq. (2) by subtracting  $n_0$  and dividing by  $n_1$  as in Eq. (9).

$$\frac{n(a_0 + a, t) - n_0}{n_1} = \sin(\omega t) \quad (9)$$

In a similar manner we can non-dimensionalize the output from Eq. (8).

$$\frac{\bar{n}(t) - n_0}{n_1} = \frac{1}{2} \sin(\omega t) + \frac{4}{\pi^2} \sum_{k=1}^{\infty} \frac{\sin(\omega t - 2\beta_k)}{(2k-1)^2} \quad (10)$$

Since the oxygen concentration and absolute pressure are proportional to one another, Eqs. (9)

and (10) are equivalent to the non-dimensionalized stimulus and indicated response pressures.<sup>8</sup> Recall that the static calibration assumes an equilibrium oxygen concentration across the layer. Under non-equilibrium conditions, as in Eq. (10), the average oxygen concentration in the layer causes an indicated pressure different than the true pressure of Eq. (9). Thus, we must compare the true pressure at the surface of the PSP to the indicated pressure via Eqs. (9) and (10), respectively. We can do this by running a computer simulation in which we step through  $\omega$  to produce the projected response of the paints in the frequency domain. The resulting amplitude ratio (ratio of the indicated to true pressure) and phase shift of such a simulation are shown in Figs. 4 and 5. In this simulation,  $\tau$  was set to one and only the first 2000 terms of the sum in Eq. (10) were used. Also included in the figures are the responses of standard 1<sup>st</sup> order and 2<sup>nd</sup> order systems. The magnitude and phase responses of a 1<sup>st</sup> order system are given in Eqs. (11) and (12).<sup>6</sup>

$$A_1(\omega) = \frac{1}{[1 + (\omega\tau)^2]^{1/2}} \quad (11)$$

$$\phi_1(\omega) = -\tan^{-1}(\omega\tau) \quad (12)$$

Similarly, for a 2<sup>nd</sup> order system (critically damped):

$$A_2(\omega) = \frac{1}{[1 + (\omega\tau)^4]^{1/2}} \quad (13)$$

$$\phi_2(\omega) = -2 \tan^{-1}(\omega\tau) \quad (14)$$

Note that to achieve the data in the amplitude and phase response graphs, we must take twenty times the log of the amplitude ratio to get the amplitude ratio in decibels (dB), and we must multiply the phase shift by 180 and divide by  $\pi$  to change from radians to degrees. For a 1<sup>st</sup> order system, the amplitude ratio has a high-frequency asymptote with slope -20 dB/decade and the phase shift levels off at -90° for large frequencies. For a 2<sup>nd</sup> order system, these values are -40 dB/decade and -180°. So, following the trends of 1<sup>st</sup> and 2<sup>nd</sup> order systems, it would appear that the response of the PSP model is that of a "1/2 order system" since the high-frequency asymptote of the amplitude ratio has a slope of -10 dB/decade and the phase shift levels off at -45° for large frequencies. However, in the neighborhood of the break point the behavior of both the amplitude ratio and the phase shift differ from what one would expect out of a "1/2 order system," namely,

$$A_{1/2}(\omega) = \frac{1}{[1 + (\omega\tau)]^{1/2}} \quad (15)$$

$$\phi_{1/2}(\omega) = -\frac{1}{2} \tan^{-1}(\omega\tau) \quad (16)$$

However, with the use of curve-fitting software, analytic functions were found which adequately fit the amplitude and phase response of this model and are detailed in Eqs. (17) - (19).

$$A_{\text{model}}(\omega) = \frac{0.1551}{[1 + (\omega\tau/15.51)]^{1/2}} \quad (17)$$

$$\phi_{\text{model}}(\omega) = -\frac{1}{2} \tan^{-1}(\omega\tau) + \frac{0.8449}{[1 + (\omega\tau/0.8968)^2]^{1/2}} - \frac{0.2446}{1 + 0.8115\gamma \exp(0.0943\gamma)} \quad (18)$$

where

$$\gamma = [\log(\omega\tau/1.423)^2]^2 \quad (19)$$

Note that the break point of a system is defined as the point where  $\omega\tau = 1$ , or, when the amplitude ratio is at -3 dB. Since  $\omega = 2\pi f$ , we then have a convenient way of calculating  $\tau$ . That is, find the frequency at the break point,  $f_{bp}$ , and then compute  $\tau = 1/2\pi f_{bp}$ . In the next section, the behavior of the model PSP system is compared to experimentally obtained PSP data by matching the break points of the model and the data.

## Results

There are many benefits to working in the frequency-domain. The first is that the experiments involved are generally periodic in time. This allows for averaging over successive periods of the data. Another way which eliminates the noise even more efficiently is to apply Wiener filtering to the data. This involves the averaging of power spectra (Fourier magnitude squared) and then subtracting off the background white noise.<sup>7</sup> Unfortunately, the frequency response involves not only the Fourier magnitude but also the phase spectrum. Simply averaging the phase spectra does not produce a good measure of the phase at high frequencies. For this reason an algorithm was developed which involves

creating a histogram for each discrete frequency bin of the phase spectrum. Each time a phase spectrum is taken, the measurement at each frequency is put into the histogram at that frequency. After several spectra have been acquired and put into the histograms, the maxima of each histogram is easily pulled out. One disadvantage of this method is that the data acquisition must be triggered on the pressure wave else the phase measurements will be uncorrelated. Fortunately, triggering the acquisition on the rising edge of the wave is simple to accomplish. In a typical experiment, one could imagine driving the pressure field using a sinusoidal function. However, such an experiment is limited in that it only provides information about a particular frequency. Fortunately again, there is a way to get more information out of a single experiment. That is, rather than using a sinusoidal pressure field, one can use a sawtooth shaped driving function which will then give information at the driving frequency and at several of the higher harmonics as presented by Carroll, et. al.<sup>8</sup> Such were the experiments performed here.

There are several questions that arise in the general use of PSP's. The first, is whether the response of the paints is invariant to the mean pressure level. That is, whether the amplitude response changes with different mean pressure levels. The second is whether the response of the paints is invariant to the magnitude of the pressure change, i.e., whether the amplitude response is a function of the peak-to-peak amplitude of a sinusoidal pressure field. The third is what effect the coating thickness has on the frequency response.

To answer the first and second questions, three successive experiments were performed on one representative sample. The thickness of the sample was  $a = 16 \mu\text{m}$  and the pressure field was driven with a 1 Hz sawtooth wave. In these tests, three different mean pressure levels were used: 50 kPa, 75 kPa, and 120 kPa. In addition, three different peak-to-peak amplitudes were used: 60 kPa, 75 kPa, and 85 kPa. The amplitude ratio and phase shift of these tests are shown in Figs. 6 and 7 respectively. Note that there is no correlation between the pressure levels used and the PSP response in either the amplitude ratio or the phase shift which confirms that the frequency response of the paints is invariant to the pressure field. Also included in Figs. 6 and 7 are comparisons of the analytical model from Eqs. (17) and (18) to the

experimental data. The value of  $\tau$  used in the equations was 0.148 seconds and came from the table in the next paragraph. Another way in which the analytical model could have been compared to the experimental data would be to perform a least-squares curve fit of the analytical model to the data with  $\tau$  as a parameter of the fit. However, since the slope of the data for frequencies above the break point is clearly not -10 dB/decade, it was felt that forcing the break points of the data and the model to occur at the same frequency was a better method of comparison. At this point it seems quite clear that the model does not fully explain the behavior of the paints. However, we speculate that this might possibly be due to oxygen absorbed into the primer layer which is then diffusing into the PSP layer from below, thus, corrupting the model. With respect to the analytical model of Eqs. (1) - (4), we would then have to replace Eq. (3) with two equations. One to represent the boundary condition at the interface between the PSP layer and the primer layer and one for the boundary condition at the interface between the primer layer and the aluminum base. We would also have to solve the diffusion equation inside the primer layer, which would have its own mass diffusion coefficient. In all, it appears that the incorporation of this speculation into the existing model would be quite complex and might not result in as simple an analytic form as the current model of Eq. (10). To check if the primer layer is indeed influencing the PSP layer, there are plans to apply the PSP layer directly to the aluminum base with no primer layer.

As to the third question, experiments were performed on four samples of the same style paint but with varying thicknesses. The thicknesses of the four samples were  $a = 6 \mu\text{m}$ ,  $11 \mu\text{m}$ ,  $16 \mu\text{m}$ , and  $20 \mu\text{m}$  with an uncertainty of  $\pm 2 \mu\text{m}$ . On each sample two tests were performed. On the  $6 \mu\text{m}$  and  $11 \mu\text{m}$  samples one test was with a 1 Hz sawtooth wave and one was with a 5 Hz sawtooth wave. For the  $16 \mu\text{m}$  and  $20 \mu\text{m}$  samples, the sawtooth wave driving frequencies were 0.1 Hz and 1 Hz. The data from each of these pairs of tests were then spliced together. The resulting amplitude ratio and phase shift diagrams are shown in Figs. 8 and 9. Note in Fig. 8 the intersection of the -3 dB line with the four amplitude ratio curves. Recall that this intersection takes place where  $\tau = 1/2\pi f_{bp}$ . The following table shows a comparison of the break frequencies  $f_{bp}$ , characteristic lifetimes  $\tau$  and the effective mass diffusivities  $D_m$  calculated from Eq. (7).

a (μm)	f <sub>bp</sub> (Hz)	τ (sec)	D <sub>m</sub> (cm <sup>2</sup> /sec)
6	7.11	0.0224	6.51 x 10 <sup>-6</sup>
11	2.71	0.0586	8.37 x 10 <sup>-6</sup>
16	1.08	0.148	7.03 x 10 <sup>-6</sup>
20	0.414	0.384	4.22 x 10 <sup>-6</sup>

The break point quite clearly shifts to lower frequencies as the thickness of the paint increases which is consistent with the analytical model. The values of  $\tau$  and  $D_m$  calculated here agree to within ten percent with another method currently being developed at the University of Florida which is based upon the response of the PSP's to a step change in pressure.<sup>4</sup> These results will be presented in a future paper.

Once the frequency response has been characterized, the development of a dynamic correction technique, i.e. transfer function, can begin. The process is fairly straightforward and is described in most any digital signal processing text.<sup>9</sup> That is, if  $A(f)$  and  $\phi(f)$  represent the magnitude and phase spectra of the frequency response (output relative to input), then  $h(t)$ , the transfer function, can be calculated

$$h_M(t) = \mathfrak{F}^{-1} \left[ \frac{1}{A(f)e^{j\phi(f)}} \right] \quad (20)$$

where  $\mathfrak{F}^{-1}$  denotes the inverse Fourier transform and  $M$  is the number of points in the sequence. Note that  $A(f)$  and  $\phi(f)$  must be the two-sided magnitude and phase spectra, not the one-sided forms shown in Figs. 4-9. That is, for  $h(t)$  real,  $A(f)$  must be symmetric about  $f_s/2$  and  $\phi(f)$  must be antisymmetric about  $f_s/2$  where  $f_s$  is the sampling frequency. Since  $h_M(t)$  is a sequence of discrete points, we will change the notation slightly and replace  $h_M(t)$  by  $h_M(i)$  where  $i$  ranges between 1 and  $M$ . Next we must select the number of terms of this sequence which best correct the input. To do this, we choose the first  $m$  points and normalize the sequence as in equation (21).

$$h_m(i) = \frac{h_M(i)}{\sum_{k=1}^m h_M(k)}, \text{ for } i = 1, \dots, m \quad (21)$$

We must then experiment with  $m$  by convolving  $h_m(i)$  with the PSP data sequence to give a corrected

PSP data sequence, and comparing to the transducer sequence until the correct number of terms is determined. This comparison is most easily done in a least-squares minimization type routine. So, if  $P_t(i)$  represents the "true" sequence, and  $P_c(i)$  represents the corrected sequence, we will vary  $m$  until we minimize

$$\text{MSE} = \frac{1}{L} \sum_{k=m}^L (P_t(k) - P_c(k))^2 \quad (22)$$

where  $L$  is the total number of points in the sequence  $P_t(i)$ , and  $P_c(i)$  is defined as

$$\begin{aligned} P_c(i) &= h_m(i) \otimes P_{\text{PSP}}(i) \\ &= \sum_{k=1}^m h_m(k) P_{\text{PSP}}(i - k) \end{aligned} \quad (23)$$

In Eq. (23)  $P_{\text{PSP}}(i)$  is the PSP data sequence and  $\otimes$  represents the convolution operation. The purpose of summing between  $m$  and  $L$  in Eq. (22) rather than from 1 to  $L$  is that the first  $m-1$  points of the sequence  $P_c(i)$  are corrupted due to the convolution process. Usually the number of necessary terms  $m$  is less than ten if the sampling rate has been properly chosen. That is, the PSP's are limited in the frequency of input to which they will respond. In the experiments performed here it was found that the PSP's were bandlimited to frequencies less than about 50 Hz. Or, above 50 Hz the PSP output was so small as to be buried in noise. So, according to Nyquist's sampling theorem, a sampling rate above 100 Hz will collect all information carried in the PSP data.<sup>9</sup> If the data is sampled at a rate much greater than this many more terms of the sequence  $h_M(i)$  will be necessary to properly correct the PSP data.

The results of this entire scheme for one such experiment are shown in Fig. 10. In this experiment the pressure in the test cell was driven by a 1 Hz sawtooth wave and the data was sampled at a rate of 128 Hz. The sample thickness was 16 μm. The corrected pressure was derived using the first six terms of the transfer function sequence. The dynamic correction scheme was then:

$$\begin{aligned} P_c(i) &= 5.119P_{\text{PSP}}(i) + 0.425P_{\text{PSP}}(i - 1) \\ &\quad - 0.962P_{\text{PSP}}(i - 2) - 1.576P_{\text{PSP}}(i - 3) \\ &\quad - 1.376P_{\text{PSP}}(i - 4) - 0.630P_{\text{PSP}}(i - 5) \end{aligned} \quad (24)$$

where  $i = 1, \dots, L$ . This type of equation is known as a linear constant-coefficient difference equation (lccde). Note that the first five data points are off the scale of the graph in Fig. 10. This graphically shows how the first  $m-1$  data points are corrupted by the correction scheme as was previously mentioned. There are three things to note about Eq. (24). First, it represents a causal correction scheme. That is, it does not depend on future data values of the PSP pressure. This is good in that the correction scheme can be run real-time in an experiment or can be run during post-processing. Second, the sum of the coefficients is unity. This must always be true for any correction scheme, else the output will be incorrectly scaled. Third, the coefficients of this scheme are dependent on the sampling rate. So, this corrector is only good for this particular type and thickness of paint sampled at 128 Hz. As can be seen in Fig. 10, this scheme corrects the PSP pressure sequence to within 5 kPa of the true value which is a great improvement over the PSP measurement alone.

### Conclusions

An investigation of the frequency response of PSP's has revealed many items of note. First, the dynamic response of the PSP's is not a function of pressure. It must therefore be assumed that the dynamic response can be completely characterized by the lumiphore and polymer binder physical properties. Second, the experimental results confirmed the trend based on the analytical solution that the square of the coating thickness has an inverse relationship to the lifetime of the paints. Third, it cannot be said for certain that the analytical model developed here completely describes the response of the PSP layers. However, this is partially due to the physical limitations of the experimental setup. The current test cell cannot produce large enough pressure fluctuations at frequencies above 50 Hz to evoke a measurable response from the PSP's. If such could be designed, the high frequency response of the PSP's might be measured and compared to the analytical model to see if the system is indeed a "1/2 order system." Finally, the dynamic correction scheme based upon experimental data presented here appears to be quite good. With this new experimental technique many phenomena such as aircraft wing flutter or shock motion in inlets may be fully analyzed with PSP's.

### Acknowledgements

Financial support of this research was provided by NASA Langley Research Center, the Florida Space Grant Consortium and the Department of Aerospace Engineering, Mechanics & Engineering Science. We would also like to thank Dr. Martin Morris of McDonnell Douglas who provided the PSP samples.

### References

1. Morris, M.J.; Donovan, J.F., Kegelman, J.T.; Schwab, S.D.; Levy, R.L.; Crites, R.C. "Aerodynamic Applications of Pressure Sensitive Paint," *ALAA Journal*, Vol. 31, 1993 p. 419.
2. Kavandi, J.; Callis, J.; Gouterman, M.; Khalil, G.; Wright, D.; Green, E.; Burns, D.; McLachlan, B. "Luminescent Barometry in Wind Tunnels," *Rev. Sci. Instrum.* 1990, Vol. 61, 1990, p. 3340.
3. McLachlan, B.G.; Kavandi, J.L.; Callis, J.B.; Gouterman, M.; Green, E.; Khalil, G.; Burns, D. "Surface Pressure Field Mapping Using Luminescent Coatings," *Experiments in Fluids*, Vol 14, 1993.
4. Carroll, B. F., Abbitt, J. D., Lukas, E. W., and Morris, M. J., "Step Response of Pressure-Sensitive Paints" *ALAA Journal*, Vol. 34, No. 3, March 1993 pp. 521-526.
5. Baron, A. E., Danielson, D. S., Gouterman, M., Wan, J. R., Callis, J. B., and McLachlan, B., "Submillisecond Response Times of Oxygen-Quenched Luminescent Coatings," *Rev. Sci. Instrum.*, Vol. 64, No. 12, Dec. 1993, pp. 3394-3402.
6. Tse, F. S., and Morse, I. E., *Measurement and Instrumentation In Engineering*, Marcel Dekker, Inc., New York, 1989.
7. Kay, S. M., *Modern Spectral Estimation*, Prentice Hall, Inc., Englewood Cliffs, NJ, 1988.
8. Carroll, B. F., Winslow, N. A., Abbitt, J. D., Schanze, K., and Morris, M., "Pressure Sensitive Paint: Application to a Sinusoidal Pressure Fluctuation," IEEE CH34827-95/0000, Proceedings of the 16th ICIASF, July 18-21, 1995, pp. 35.1-35.6.
9. Oppenheim, A. V., and Schafer, R. W., *Discrete-Time Signal Processing*, Prentice Hall, Inc., Englewood Cliffs, NJ, 1989.



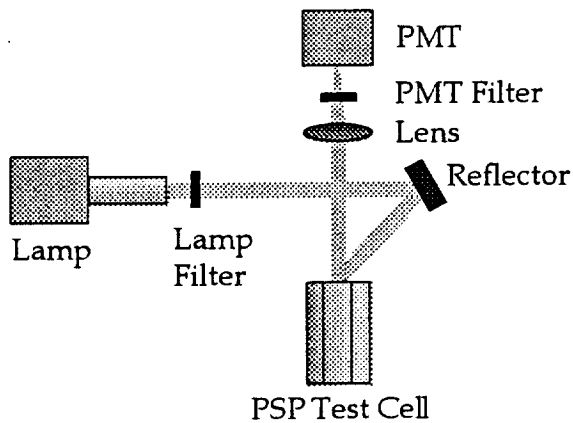


Fig. 1 Experimental setup diagram.

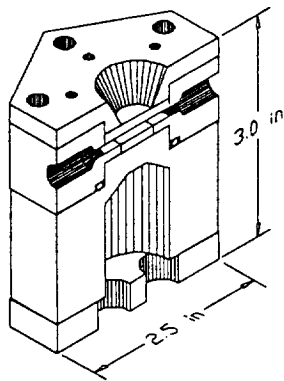


Fig. 2 Cut view of PSP test cell.

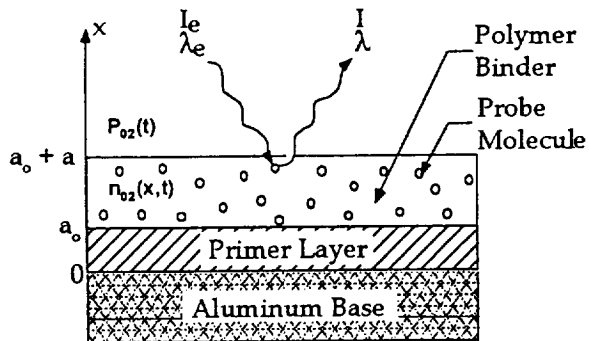


Fig. 3 Side view of PSP sample including coordinate system used in diffusion model.

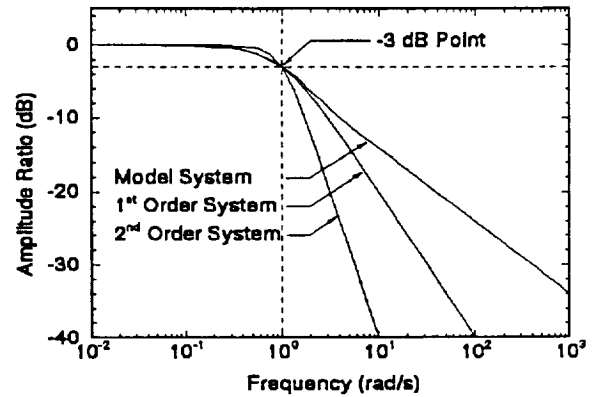


Fig. 4 Amplitude response of model system with comparison to 1<sup>st</sup> order and 2<sup>nd</sup> order systems.

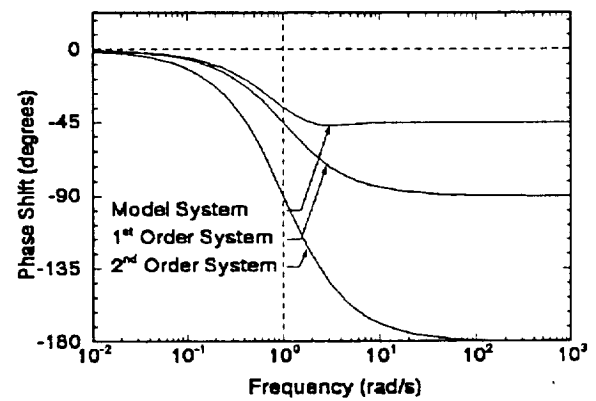


Fig. 5 Phase response of model system with comparison to 1<sup>st</sup> order and 2<sup>nd</sup> order systems.

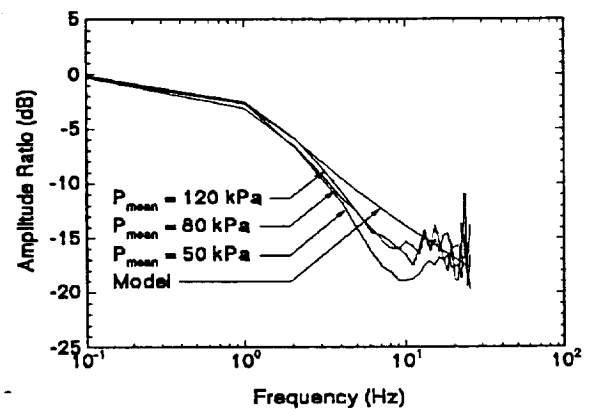


Fig. 6 Amplitude response of 16 $\mu$ m PSP sample for three different mean pressure levels.

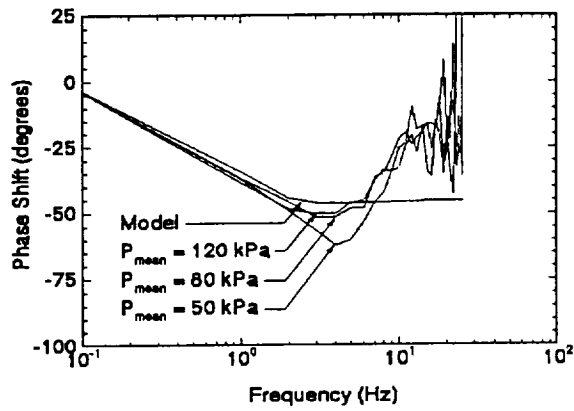


Fig. 7 Phase response of 16  $\mu\text{m}$  PSP sample for three different mean pressure levels.

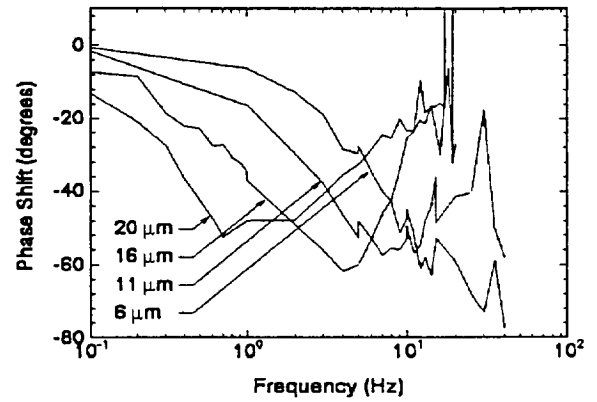


Fig. 9 Phase response of four different thickness PSP samples.

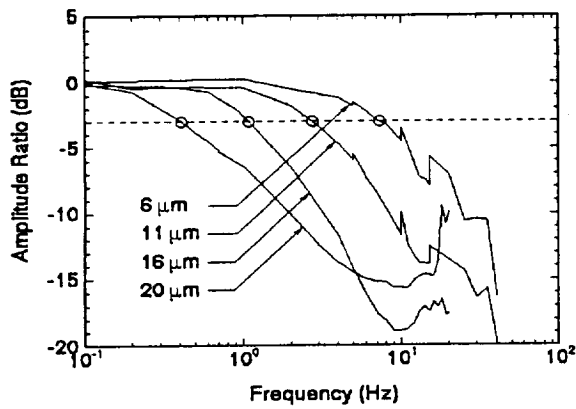


Fig. 8 Amplitude response of four different thickness PSP samples. The circles denote the break point of each response curve where  $\omega\tau = 1$ .

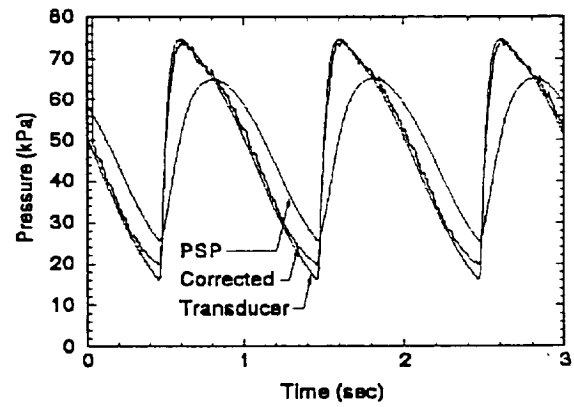


Fig. 10 Results of correction scheme for a 1 Hz sawtooth wave input and 16  $\mu\text{m}$  thick sample.